



Sources of humic-like substances in the Pearl River Delta, China: positive matrix factorization analysis of PM_{2.5} major components and source markers

B. Y. Kuang¹, P. Lin^{1,*}, X. H. H. Huang², and J. Z. Yu^{1,2}

¹Department of Chemistry, Hong Kong University of Science & Technology, Clear Water Bay, Kowloon, Hong Kong SAR, China

²Institute of Environment, Hong Kong University of Science & Technology, Clear Water Bay, Kowloon, Hong Kong SAR, China

* now at: Environmental Molecular Sciences Laboratory, Pacific Northwest National Laboratory, Richland, Washington, 99532, USA

Correspondence to: J. Z. Yu (jian.yu@ust.hk)

Received: 15 August 2014 – Published in Atmos. Chem. Phys. Discuss.: 16 September 2014

Revised: 28 December 2014 – Accepted: 25 January 2015 – Published: 24 February 2015

Abstract. Humic-like substances (HULIS), the hydrophobic part of water-soluble organic carbon (WSOC), account for a significant fraction of PM_{2.5} mass. Their source studies are so far largely qualitative. In this study, HULIS and WSOC were determined in 100 PM_{2.5} samples collected in 2009 at an urban site (Guangzhou) and a suburban site (Nansha) in the Pearl River Delta in South China. The annual average concentration of HULIS was 4.83 and 4.71 μg m⁻³, constituting 8.5 and 10.2 % of the PM_{2.5} mass, while HULIS-C (the carbon component of HULIS) contributed 48 and 57 % of WSOC at the two sites, respectively. HULIS were found to correlate with biomass burning (BB) tracers (i.e., levoglucosan and K) and secondary species (e.g., SO₄²⁻ and NH₄⁺), suggesting its association with BB emissions and secondary formation processes. Sources of HULIS were investigated using positive matrix factorization analysis of PM_{2.5} chemical composition data, including major components and source markers. In addition to secondary formation process and BB emissions, residual oil combustion related to shipping was identified for the first time as a significant source of HULIS. Secondary formation process contributed the most, accounting for 49–82 % of ambient HULIS at the two sites in different seasons. BB emissions contributed a seasonal average of 8–28 %, with more contributions observed in the winter months (November–February) due to crop residue burning during harvest season. Residual oil combustion was re-

vealed to be an important source at the suburban site in summer (44 % of HULIS-C) due to its proximity to one of the ports and the shipping lane in the region. Vehicle emissions were found to contribute little to HULIS, but had contributions to the hydrophilic WSOC fraction. The contrast in contributions from different combustion sources to HULIS and hydrophilic WSOC suggests that primary sources of HULIS are linked to inefficient combustion. This source analysis suggests further study of HULIS be focused on secondary formation process and source characteristics of HULIS from BB and residual oil combustion.

1 Introduction

Humic-like substances (HULIS) are a mixture of organic species extracted from atmospheric aerosol particles with characteristics similar to humic and fulvic acids (Graber and Rudich, 2006). It is operationally defined by procedures used for its isolation from the bulk water-soluble aerosol components by removing inorganic salts and low-molecular weight hydrophilic organic compounds (e.g., oxalate). HULIS are therefore the hydrophobic part of water-soluble organic carbon (WSOC). Solid phase extraction (SPE) methods have been widely used to isolate HULIS (e.g., Varga et al., 2001; Lin et al 2010a, 2010b). The advantage of SPE is the re-

removal of inorganic ions and the collection of the organic fraction, facilitating subsequent characterization of the chemical and physical properties of HULIS. Other methods have also been utilized, such as capillary electrophoresis (Havers et al., 1998a), ultrafiltration (Havers et al., 1998b), ion-exchange chromatography (Decesari et al., 2000), and size-exclusion chromatography (Krivacsy et al., 2000; Samburova et al., 2005a, b).

HULIS are a significant component of particulate matter (PM) (Lin et al., 2010a). It accounted for around half or more of WSOC in previous studies (e.g., Krivacsy et al., 2008). Due to its abundant presence and its affinity for water, HULIS play an important role in the atmosphere by affecting the hygroscopic growth of aerosols and reducing surface tension (Kiss et al., 2005; Dinar et al., 2006; Graber and Rudich, 2006). HULIS could also be important contributors to light absorption by particles in the atmosphere (Hoffer et al., 2006; Lukacs et al., 2007). More recently, HULIS have been demonstrated to be redox-active. It catalyzes the generation of reactive oxygen species under simulated physiological conditions, thereby likely contributing to PM-induced health effects (Lin and Yu, 2011; Verma et al., 2012).

Previous studies have identified biomass burning (BB) (Mayol-Bracero et al., 2002; Lukacs et al., 2007; Lin et al., 2010b) and secondary formation (Altieri et al., 2008; El Haddad et al., 2011; Lin et al., 2010a) as important sources of HULIS. One study also reported that HULIS could have a marine source (Cavalli et al., 2004). The molecular composition of HULIS was also studied using ultrahigh resolution mass spectrometer (e.g., Wozniak et al., 2008; Lin et al., 2012a, b; Yassine et al., 2012). Through composition study, it was confirmed that biomass burning and secondary formation process were sources of HULIS (Lin et al., 2012a). However, to the best of our knowledge, there is not yet a quantitative source apportionment study of HULIS.

Positive matrix factorization (PMF) is a multivariate factor analysis model that has been widely used for source apportionment of ambient samples. There are a number of studies using PMF to identify and apportion sources of ambient aerosols in Hong Kong (Lee et al., 1999; Yuan et al., 2006a, b; Hu et al., 2010) and many more studies in other locations around the world (e.g., Maykut et al., 2003; Kim and Hopke, 2004; Liu et al., 2005; Shrivastava et al., 2007; Wagener et al., 2012). The objective of this study is to identify major sources of HULIS and quantify their contributions in PM_{2.5} samples in the Pearl River Delta (PRD). The approach taken is through PMF analysis of PM_{2.5} chemical composition data including inorganic and organic tracers for key sources. The tracers of the biomass burning, vehicular emission, ship emission, and dust are included in PMF, because PMF relies on source tracers to associate resolved factors with known sources or processes.

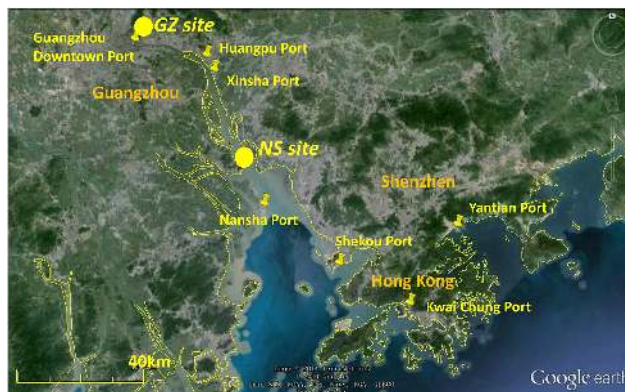


Figure 1. Location of the Guangzhou (GZ) and Nansha (NS) sampling sites.

2 Experimental section

2.1 Aerosol sampling

Ambient aerosol samples were collected at an urban site (GZ: Guangzhou) and a suburban site (NS: Nansha) in the PRD (Fig. 1). The GZ site (23°7′51.08″ N, 113°17′51.19″ E) is located on the roof of the Guangdong Meteorology Bureau building in downtown Guangzhou. The NS site (22°45′08.90″ N, 113°36′09.17″ E) is located in the middle of the PRD, 50 km south of the GZ site and ~15 km north of Nansha Port. NS is situated at the estuary of the Pearl River on the shipping lane from Hong Kong/Shenzhen to Guangzhou Downtown Port (Fig. 1).

Twenty-four-hour PM_{2.5} sampling was conducted at each site once every 6 days throughout the year of 2009. A MetOne Speciation Air Sampling System (SASS) medium volume sampler was used at each site to collect aerosols onto one Teflon, one Nylon and three pre-baked quartz filters through five separate sampling channels. A high-volume aerosol sampler (TE-6070V-BL, Tisch Environmental Inc., USA) was employed at each site to collect PM_{2.5} samples on prebaked quartz filters. The Teflon, nylon, and quartz filters from the mid-volume samplers were used for gravimetric measurement, water-soluble ions, and EC/OC (elemental carbon/organic carbon) analysis, respectively (Huang et al., 2014). Quartz filters from the high-volume samplers were used for determination of HULIS, WSOC, and organic source tracers.

2.2 Chemical analysis

Chemical species analyzed in the PM_{2.5} samples include nine ionic species (Cl⁻, NO₃⁻, SO₄²⁻, oxalate, Na⁺, NH₄⁺, K⁺, Mg²⁺, and Ca²⁺), EC, OC, elements (Al, Si, K, Ca, Ti, V, Mn, Fe, Ni, Zn, Pb), HULIS, WSOC, three sugar compounds (levoglucosan, mannosan, and galactosan), and hopanes. Ionic species were quantified using an ion chro-

matography (IC) system (DX500, Dionex, Sunnyvale, CA, USA), and the experimental details were reported in our earlier papers (Yang et al., 2005; Lin et al., 2010a). EC and OC were determined using a thermal/optical transmittance aerosol carbon analyzer (Sunset Laboratory, Tigard, OR, USA) and the analysis protocol followed the ACE-Asia protocol, which is derived from the better known NIOSH protocol (Wu et al., 2012). Elements were measured using an X-ray fluorescence (XRF) spectrometer (Huang et al., 2014).

For the analysis of WSOC and HULIS, portions of the quartz filters were extracted by sonication in ultrapure water ($> 18 \text{ M}\Omega \text{ cm}$, Barnstead Nanopure ultrapure water system, APS Water Services Corp., USA) with the ratio of 1 mL water per 1 cm^2 filter. The extracts were filtered with a $0.45 \mu\text{m}$ Teflon filter (Millipore, Billerica, MA, USA) to remove insoluble materials before analysis. The WSOC content was determined using a TOC analyzer equipped with a non-dispersive infrared (NDIR) detector (Shimadzu TOC-V_{CPH}, Japan). The detector response was calibrated with authentic standard of sucrose (sucrose standard was purchased from Fisher Scientific UK Limited, Loughborough, UK). Water-insoluble OC (WISOC) is then calculated to be the difference between OC and WSOC. The quantification of HULIS was described in detail in our previous studies (Lin et al., 2010a, 2010b). Briefly, the aerosol water extract was acidified with HCl to $\text{pH} \approx 2$, then loaded to the SPE cartridge (Oasis HLB, $30 \mu\text{m}$, 60 mg/cartridge , Waters, USA). HULIS were retained on the SPE cartridge while the majority of inorganic ions, low molecular weight organic acids, and sugars were not retained. The sorbent was rinsed with 2 mL ultrapure water, and the HULIS fraction was then eluted from the SPE cartridge with 1.5 mL methanol containing 2% (*w/w*) NH_3 . The HULIS eluate was evaporated to dryness under a gentle stream of nitrogen gas and re-dissolved in 1.0 mL of water, followed by detection using an evaporative light scattering detector (ELSD). Routine calibration of the ELSD was carried out using standard solutions of SRFA (Suwannee River Fulvic Acid, International Humic Substances Society) up to 250 mg L^{-1} (the upper limit of the ELSD dynamic range). Since HULIS are the hydrophobic part of WSOC, we term the difference between WSOC and HULIS-C (the carbon content of HULIS) to be hydrophilic WSOC, abbreviated as WSOC_h hereafter. HULIS-C was calculated from HULIS mass divided by a factor of 1.9, as determined in previous studies (Kiss et al., 2002; Lin et al., 2010b). We note that HULIS-C in concentration unit of $\mu\text{g C m}^{-3}$, instead of HULIS mass concentration ($\mu\text{g m}^{-3}$), was used as input in the PMF analysis and consequently the source apportionment results are in reference to HULIS-C. Using HULIS-C allows the easy derivation of WSOC_h data from WSOC and HULIS-C and subsequently the investigation of WSOC_h sources.

The concentrations of levoglucosan, mannosan, and galactosan were measured by high-performance anion-exchange chromatography (HPAEC) with a pulsed amperometric de-

tection (PAD) method (Engling et al., 2006). The measurement was carried out on a Dionex DX-500 series ion chromatograph (Sunnyvale, CA, USA), consisting of a LC30 Chromatography Oven, a GP40 Gradient Pump, and an ED40 Electrochemical Detector (with an electrochemical cell and a conventional gold electrode). The separation was achieved on a Dionex CarboPac PA10 analytical column ($4 \times 250 \text{ mm}$) with aqueous sodium hydroxide (NaOH) as eluent at a flow rate of 0.5 mL min^{-1} (Engling et al., 2006). The chromatographic conditions were 10% of aqueous solution containing 180 mM NaOH (A) and 90% of ultrapure water (B) for 10 min; eluate A increased from 10 to 70% in 20 min, then from 70 to 100% in 0.1 min and maintained at 100% for 9 min to wash the column. At the end of the analysis cycle, eluate A was decreased to 10% in 0.1 min and kept at 10% for 14 min to condition the column for the next sample. The detector was operated in integrating amperometric mode and its response was calibrated by authentic standards of the three sugars. Levoglucosan was purchased from Sigma-Aldrich Inc. (St. Louis, MO, USA), mannosan from Toronto Research Chemicals Inc. (North York, ON, Canada), and galactosan from J&K Scientific (USA).

Hopanes, together with other nonpolar organic compounds (i.e., alkanes, polycyclic aromatic compounds), were quantified using a method that couples in-injection port thermal desorption with gas Chromatography/mass spectrometric detection (TD-GC/MS) (Agilent 7890A GC/5975C MS). The experimental details and method evaluation through comparison with solvent extraction GC-MS analysis are described in our previous papers (Ho and Yu, 2004; Ho et al., 2008). A 2 cm^2 filter punch from each filter collected with the high-volume samplers was removed and used in the TD-GC/MS analysis. The separation was achieved using an HP-5 ms capillary column ($30 \text{ m} \times 0.25 \text{ mm} \times 0.25 \mu\text{m}$, J&W Scientific, Folsom, CA, USA). Two hopanes, C $30\alpha\beta$ -hopane (abbreviated as hopane hereafter) and C $29\alpha\beta$ -hopane (norhopane), are used in this work as vehicular emission tracers.

2.3 PMF analysis

EPA PMF 3.0 (Norris et al., 2008; Kim and Hopke, 2007; Kim et al., 2010) was used in this study. A total of 27 fitting species are used as input observable parameters, including HULIS-C, WSOC_h, 3 sugar species (levoglucosan, mannosan, and galactosan), hopane, norhopane, EC, OC, 7 major ions (SO_4^{2-} , NO_3^- , Cl^- , oxalate, NH_4^+ , Na^+ , and Mg^{2+}), and 11 elements (Al, Si, K, Ca, Ti, V, Mn, Fe, Ni, Zn, Pb). Elements K and Ca measured by XRF were used as PMF inputs because of better accuracy than ionic K^+ and Ca^{2+} measured with the IC system. Levoglucosan is a tracer highly specific for BB emissions (Simoneit et al., 1999; Nolte et al., 2001; Engling et al., 2006). It has been widely used to estimate the contributions of BB emission to ambient aerosols in source apportionment studies (e.g., Wang et al., 2007; Holden et

al., 2011; Harrison et al., 2012). Hopane and norhopane are specific tracers for vehicle emissions (e.g., Simoneit et al., 1984). Sulfate is a marker species for secondary formation processes (e.g., Yu et al., 2005; Huang et al., 2006). Na^+ and Mg^{2+} are tracers for sea salt aerosols. Ni and V are often used as tracers of ship emissions (Guo et al., 2009; Mooibroek et al 2011). Al, Ca and Fe are components of crustal materials, tracking dust aerosols (Zota et al 2009; Khan et al 2012).

The uncertainties for individual species were calculated as $(S_{ij} + \text{DL}/3)$, where S_{ij} is the analytical uncertainty of the species j in i th sample and DL is method detection limit (Reff et al., 2007). For data below their respective DLs, the concentration was set to be $0.5 \times \text{DL}$ and the corresponding uncertainty was set at $(5/6) \times \text{DL}$ (Polissar et al., 1998; Norris et al., 2008).

3 Results and discussion

3.1 Overview of the concentrations of aerosol speciation

Table 1 shows the summary statistics for the concentrations of species measured for the PMF analysis in a total of 100 samples collected in 2009. Among them, 51 were collected from GZ and 49 were from NS. The individual sampling days are listed in Table S1, together with the concentrations of $\text{PM}_{2.5}$, WSOC and HULIS in each sample.

3.1.1 Major $\text{PM}_{2.5}$ components

Annual average $\text{PM}_{2.5}$ concentration was higher in GZ ($56 \mu\text{g m}^{-3}$) than NS ($44 \mu\text{g m}^{-3}$). They were lower than measurements obtained for the period of July 2007–August 2008 (GZ: $78 \mu\text{g m}^{-3}$, NS: $66 \mu\text{g m}^{-3}$) (Lin et al., 2010b). Seasonally, $\text{PM}_{2.5}$ was higher in winter (GZ: $68 \mu\text{g m}^{-3}$, NS: $57 \mu\text{g m}^{-3}$) than summer (GZ: $39 \mu\text{g m}^{-3}$, NS: $25 \mu\text{g m}^{-3}$) (Fig. S5). Sulfate and organic matter (OM) were the two most abundant components. OM accounted for one-fourth to one-third of $\text{PM}_{2.5}$ mass in summer and winter (Fig. S5), indicating the importance of sources analysis of OM. Sulfate, ammonium and oxalate are mainly from secondary formation processes. Their average concentrations were comparable at GZ and NS. The average concentration of EC was higher in GZ ($2.89 \pm 1.66 \mu\text{gC m}^{-3}$) than in NS ($2.12 \pm 1.11 \mu\text{gC m}^{-3}$). This is consistent with the characteristics of the two sites and the fact that EC is mainly from vehicular emissions in urban areas. GZ is an urban site and the influence of vehicular emissions is more prominent than NS, the suburban site.

3.1.2 WSOC and HULIS

The concentrations of OC and WSOC were both higher at GZ than NS (Table 1). Annual average concentrations of OC

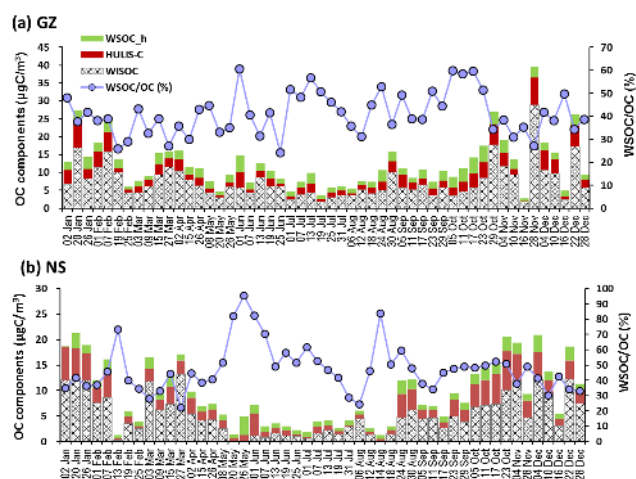


Figure 2. Spatial and temporal variation of OC fractions (i.e., HULIS-C (HULIS-carbon), WSOC_h (hydrophilic water-soluble organic carbon), WISOC (water-insoluble organic carbon)) shown as stacked bars throughout the sampling year 2009. Data of the percent of WSOC in OC are shown as line curves.

were 12.22 and $9.13 \mu\text{gC m}^{-3}$ in GZ and NS, and average concentrations of WSOC were 4.86 and $3.94 \mu\text{gC m}^{-3}$ in GZ and NS, respectively. Figure 2 shows the temporal variation of the three sub-components of OC (i.e., WSOC_h, HULIS-C, and WISOC) and the fraction of WSOC in OC. WSOC was a significant fraction of OC. On annual average, WSOC made up $41.1 \pm 9.3\%$ of OC in GZ and $47.1 \pm 15.6\%$ of OC in NS. The slightly higher WSOC proportion at NS than GZ was consistent with their suburban and urban location characteristics, respectively. NS as a suburban site is a receptor site for urban pollution. Aerosols arriving at NS have undergone a certain degree of atmospheric processing; thus, OC in the aerosols would be more oxidized and more of the OC fraction would become water-soluble. As such, WSOC/OC would be expected to be higher at NS than the urban site GZ. Seasonal variation of WSOC was observed for both sites, as shown in the time series plots of the two components of WSOC (i.e., HULIS-C and WSOC_h) (Fig. 2): WSOC was generally higher in autumn and winter (GZ seasonal averages, 5.95 and $6.01 \mu\text{gC m}^{-3}$; and NS, 5.32 and $4.96 \mu\text{gC m}^{-3}$) than spring and summer (GZ seasonal averages, 4.34 and $3.56 \mu\text{gC m}^{-3}$; and NS, 3.95 and $2.52 \mu\text{gC m}^{-3}$). Two winter days (16 November and 16 December) were exceptional, with lower concentrations of $\text{PM}_{2.5}$, OC and WSOC as a result of rain events. The variation of WSOC_h and WISOC among different samples will be discussed later in this paper (Sect. 3.2.4).

Unlike OC and WSOC that exhibit a concentration gradient between GZ and NS, the concentrations of HULIS were similar at both sites (Table 1). Annual average concentrations of HULIS were 4.83 and $4.71 \mu\text{g m}^{-3}$ in GZ and NS, respectively. The lack of an urban–suburban gradient in HULIS concentration indicates that nonurban sources dom-

Table 1. Statistic summary for the ambient concentrations of major aerosol constituents, HULIS, elements and organic tracer compounds used in the PMF analysis.

Species name	GZ mean \pm standard deviation	GZ min–max	NS mean \pm standard deviation	NS min–max
PM _{2.5} ($\mu\text{g m}^{-3}$) and carbon fractions ($\mu\text{gC m}^{-3}$)				
PM _{2.5}	56 \pm 30	8–132	44 \pm 27	4–103
OC	12.2 \pm 7.1	2.7–39.6	9.1 \pm 6.0	1.4–21.4
WSOC	4.9 \pm 2.5	1.0–10.7	3.9 \pm 2.5	1.0–10.4
HULIS	4.8 \pm 3.4	0.1–14.4	4.7 \pm 3.6	0.6–14.5
WSOC _h	2.31 \pm 0.98	0.88–4.63	1.46 \pm 0.80	0.10–3.66
WISOC ²	7.4 \pm 5.0	1.8–28.9	5.2 \pm 3.9	0.2–13.4
EC	2.9 \pm 1.7	1.0–11.9	2.1 \pm 1.1	0.2–4.6
Ions ($\mu\text{g m}^{-3}$)				
Na ⁺	0.39 \pm 0.25	BD–1.26 ³	0.39 \pm 0.21	0.10–1.02
NH ₄ ⁺	6.8 \pm 4.2	0.6–19.4	5.5 \pm 3.6	0.5–13.2
Mg ²⁺	0.061 \pm 0.060	BD–0.336	0.043 \pm 0.027	BD–0.142
Cl ⁻	1.2 \pm 1.0	BD–4.4	1.2 \pm 1.2	BD–5.2
nitrate	6.7 \pm 6.3	0.6–29.3	4.8 \pm 4.4	0.4–18.9
sulfate	13.4 \pm 6.8	1.4–27.3	12.2 \pm 7.2	2.4–30.5
oxalate	0.37 \pm 0.17	BD–0.81	0.41 \pm 0.17	BD–0.78
Trace elements ($\mu\text{g m}^{-3}$)				
Al	0.49 \pm 0.63	0.06–4.68	0.37 \pm 0.35	0.05–2.25
Si	0.9 \pm 1.5	0.1–11.4	0.68 \pm 0.83	0.06–5.50
K	0.91 \pm 0.57	0.22–2.89	0.78 \pm 0.62	0.05–2.22
Ca	0.23 \pm 0.25	0.03–1.85	0.15 \pm 0.13	0.03–0.70
Ti	0.036 \pm 0.047	0.005–0.351	0.031 \pm 0.029	0.002–0.166
V	0.0154 \pm 0.0092	BD–0.0383	0.0232 \pm 0.0096	0.0069–0.0545
Mn	0.048 \pm 0.027	BD–0.124	0.033 \pm 0.019	BD–0.091
Fe	0.49 \pm 0.48	0.09–3.54	0.30 \pm 0.26	0.03–1.63
Ni	0.0085 \pm 0.0041	BD–0.0204	0.0099 \pm 0.0038	0.0036–0.0189
Zn	0.38 \pm 0.20	0.07–1.01	0.27 \pm 0.17	BD–0.67
Pb	0.126 \pm 0.070	0.019–0.363	0.090 \pm 0.068	BD–0.313
Organic tracers (ng m^{-3})				
levoglucosan	115 \pm 90	18–366	75 \pm 79	3–336
mannosan	15 \pm 13	3–56	11 \pm 11	BD–43
galactosan	6.7 \pm 6.1	BD–26.3	5.6 \pm 5.0	BD–21.5
norhopane	1.5 \pm 1.0	0.3–4.2	0.43 \pm 0.26	0.06–1.48
hopane	1.62 \pm 0.94	0.36–4.47	0.68 \pm 0.35	0.16–2.17

¹ A total of 100 samples were included for the calculation of the statistic summary, excluding two samples (GZ 26 January, NS 26 January) not used in the PMF due to extremely high concentration of biomass burning tracers.

² WISOC: water-insoluble organic carbon.

³ BD: below detection limit.

inated ambient HULIS. This finding was consistent with results from our previous study (Lin et al., 2010a), where the annual average HULIS concentration in the suburban site NS was higher than Tsuen Wan (an urban site in Hong Kong) in year 2007–2008. The difference in spatial variation of HULIS and WSOC indicates HULIS and the rest of WSOC may differ in their major contributing sources.

The annual contribution of HULIS to PM_{2.5} was significant, 8.5 \pm 3.5 % and 10.2 \pm 4.5 % in GZ and NS, respectively. In our previous study (Lin et al., 2010a), the annual av-

erage HULIS / PM_{2.5} ratio was \sim 10 % at both NS and Tsuen Wan for a 1-year period from July 2007 to August 2008. The similar results obtained in this work confirm that HULIS are abundant in PM_{2.5}. The fraction of HULIS-C in WSOC was fairly stable across all the samples at these two sites: 48 \pm 13 % for GZ and 57 \pm 16 % for NS. These results are in broad agreement with other studies showing that HULIS-C accounts for about half of WSOC (Krivacsy et al., 2008 and references therein).

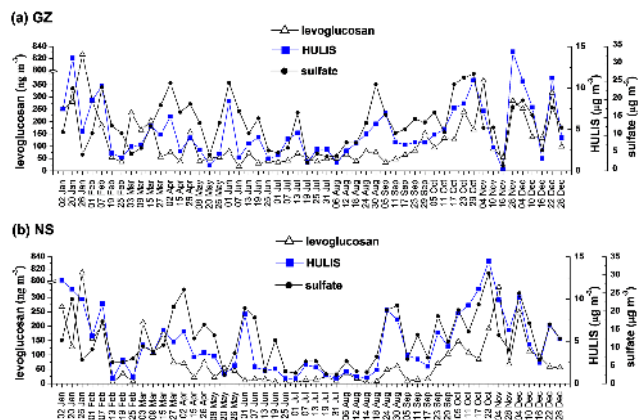


Figure 3. Spatial and temporal variation of HULIS, levoglucosan, and sulfate throughout the sampling year 2009.

3.1.3 Biomass burning tracer compounds

The yearly average concentrations of levoglucosan were 115 and 75 ng m⁻³ in GZ and NS, respectively, which means that the influence of BB emissions was more intense in GZ. Similar temporal variations were observed in both locations (Fig. 3). January to March and November to December were the periods when biomass burning was intense, with levoglucosan concentration usually higher than 50 ng m⁻³ and the average concentration was 216 ng m⁻³ at GZ, and 166 ng m⁻³ at NS. The levoglucosan concentrations were high because, during the harvest season, BB in the form of agricultural waste combustion emits large amount of aerosols into the atmosphere (Wang et al., 2007). From April to August, BB activities were reduced, and levoglucosan concentration was usually around 50 ng m⁻³ in GZ, and below 25 ng m⁻³ in NS. Wash-out of particles by increased precipitation in summer may also be an important reason for decrease of levoglucosan concentration. Ding et al (2012) reported similar temporal variation of levoglucosan in the PRD region in 2008, with a summer average of 81.0 ng m⁻³ and an average of 310 ng m⁻³ in autumn and winter.

Two samples of very high levoglucosan concentration (> 800 ng m⁻³) were observed: 827 and 814 ng m⁻³ in GZ and NS respectively on January 26. The two isomers, mannosan and galactosan, were also higher on that day than all the other samples (Fig. S1). In addition, elemental K was 3.19 and 5.25 μg m⁻³ in GZ and NS respectively, the highest among all sampling days. High concentrations of all these BB tracers suggest that there may be local BB activities on that day. That day was Chinese New Year, and we suspect festival-related activities (e.g., fireworks) could also make significant contributions to PM_{2.5}.

The concentration level of levoglucosan was strongly influenced by air mass origin. For all the sampling days, 96 h air mass back trajectories (Draxler and Ralph, 2011) were calculated using the NOAA HYSPLIT model ([| Location | X-axis | Y-axis | Equation | R ² |
|----------|------------------------------------|-----------------------------|--------------------|----------------|
| GZ | levoglucosan \(ng m ⁻³ \) | HULIS \(μg m ⁻³ \) | \$y = 0.03x + 1.66\$ | 0.53 |
| | sulfate \(μg m ⁻³ \) | HULIS \(μg m ⁻³ \) | \$y = 0.35x + 0.15\$ | 0.49 |
| NS | levoglucosan \(ng m ⁻³ \) | HULIS \(μg m ⁻³ \) | \$y = 0.03x + 2.19\$ | 0.53 |
| | sulfate \(μg m ⁻³ \) | HULIS \(μg m ⁻³ \) | \$y = 0.40x - 0.16\$ | 0.63 |](http://www.</p>
</div>
<div data-bbox=)

Figure 4. Correlation of HULIS with levoglucosan and sulfate.

arl.noaa.gov/HYSPLIT.php). They were classified into three categories: marine, continental, and transitional, according to whether their routes traveled over the South China Sea, the continent, or in-between. A total of 25 sampling days fell in the marine air mass category, 12 sampling days in the continental air mass category and 16 sampling days in the transitional air mass category. The average concentration of levoglucosan was generally lower on “marine days” (51 and 19 ng m⁻³ in GZ and NS, respectively) than “continental days” (222 and 179 ng m⁻³ in GZ and NS, respectively).

Levoglucosan, mannosan and galactosan are isomers co-emitted from biomass burning. The obvious correlations of these three species ($R^2 > 0.80$, Fig. S1) confirm similar sources of the three isomers.

3.2 Source identification and apportionment

3.2.1 Interspecies relationships between HULIS and other PM_{2.5} constituents

Interspecies relationships between HULIS and other PM_{2.5} constituents were examined to facilitate identification of HULIS sources and the coefficients of correlation (R^2) are listed in Table S2. HULIS show moderate positive correlation ($R^2 \geq 0.4$) with the BB tracers and with the secondary inorganic species (i.e., SO₄²⁻, NO₃⁻, and NH₄⁺). The correlations of HULIS with levoglucosan and sulfate are also displayed in Fig. 4. Such positive correlation relationships are consistent with the similar temporal variation trends seen in the time series plots of HULIS, levoglucosan and sulfate (Fig. 3). The temporal variation trend of HULIS are roughly similar to, but not exactly the same as, that of levoglucosan (Fig. 3). In winter, the trends of levoglucosan and HULIS were similar; when levoglucosan increased, HULIS also increased, indicating biomass burning was an important source for HULIS in winter. But throughout the summer when lev-

oglucosan was continuously low, HULIS increased significantly on 1 June and rose again in mid-August and maintained at an elevated level at both GZ and NS. In comparison, HULIS tracked sulfate well in summer as well as in winter. This indicates that secondary formation process is an important source of HULIS, especially in summer when biomass burning emissions were very low. In contrast, HULIS have low correlation with vehicle emission tracers (norhopane and hopane, R^2 are 0.19–0.38), dust elements (e.g., Al, Si, Ca, Fe, R^2 are 0.01–0.28), and ship emission tracers (V and Ni, R^2 are 0.01–0.11), suggesting that they may be less important sources of HULIS.

3.2.2 Determination of factors and source identification in PMF analysis

The PMF analysis was based on the combined data set of 100 samples at GZ and NS. The day 26 January, when levoglucosan was over 800 ng m^{-3} at both sites, was excluded from the PMF input in order not to distort the result of source apportionment.

Two methods were used to determine the number of factors (source profiles). First, the IM value (maximum individual column mean), i.e., the maximum mean of the scaled residual of each species, was calculated for all the n samples (Lee et al., 1999):

$$\text{IM} = \max_{j=1,\dots,m} \left(\frac{1}{n} \sum_{i=1}^n \frac{e_{ij}}{s_{ij}} \right), \quad (1)$$

where e_{ij} is the residual of the concentration of j th species in the i th sample and s_{ij} is the input uncertainty of the j th species' concentration of the i th sample. IM indicates the least fit species. If IM drops dramatically when the number of factors is increased by 1, it indicates that the larger number of factors is more appropriate. For our data set, IM dropped dramatically when the number of factors increased from 5 to 6, and dropped slightly when the factor number was further increased from 6 to 9 (Fig. S2). Thus, the more suitable number of factors should be higher than 5.

The interpretability of the source profile and explained variation (EV) was another criterion, and this criterion was regarded as a key basis for determining the number of factors (Liu et al., 2005; Shrivastava et al., 2007; Wang et al., 2012). Five to nine factors were tested and the six-factor solution was found to be optimum, yielding the most reasonable source profiles. The six-factor solution was verified to be stable through performing 100 bootstrap runs, as more than 88 % of the runs produced the same factors. The EV profiles of the six factors are shown in Fig. 5. They are associated with the following six sources: (1) dust as signified by the dominant presence of Al, Si, Ca, Fe, and Ti; (2) chloride and nitrate dominant source; (3) mixed ship emissions and sea salt, indicated by the dominance of Na^+ , Mg^{2+} , V, and Ni; (4) secondary sulfate formation process indicated

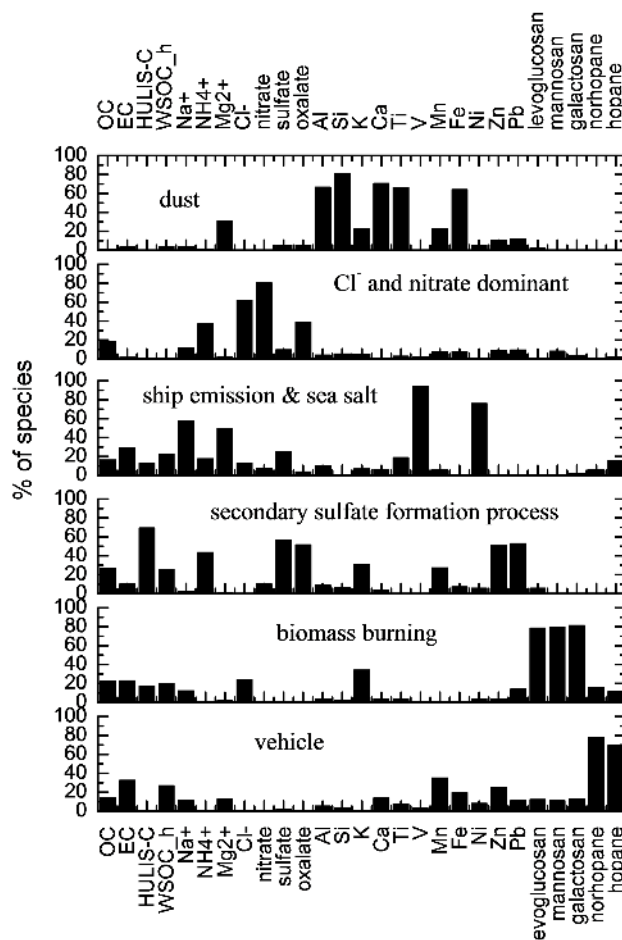
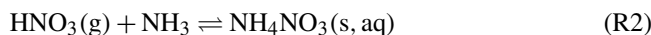
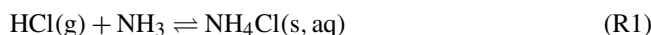


Figure 5. Explained variation of the factors apportioned by PMF.

by the dominant presence of SO_4^{2-} , NH_4^+ , and oxalate; (5) biomass burning source indicated by the three anhydrosugars and K; (6) vehicle emissions identified by EC, hopane, and norhopane. For the chloride and nitrate dominant source, 37 % of NH_4^+ is present in this factor. In this data set, chloride is moderately correlated with NH_4^+ ($R^2 = 0.31$ at GZ and 0.30 in NS). Considering this, we suggest that this factor is possibly associated with the following partitioning reactions:



The interpretability of the resolved PMF factors is also examined by inspecting the apportionment of the major $\text{PM}_{2.5}$ components (EC, OC, SO_4^{2-} , NO_3^- , and NH_4^+) in the six resolved factors. The factor contributions to individual major $\text{PM}_{2.5}$ components were averaged for each site and presented and compared with the observed concentrations in Table S3.

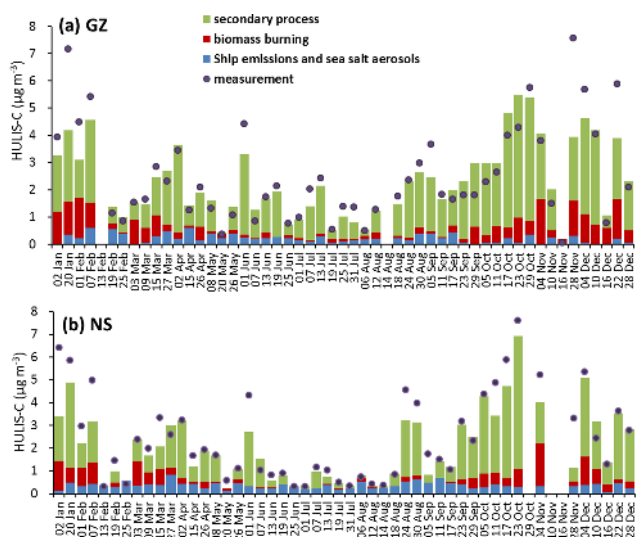


Figure 6. Spatial and temporal variation of source contributions by each factor for HULIS-C.

The modeled average concentrations of these major species deviate less than 7 % from the measured values. The apportioned source categories for the different major components are overall reasonable. Take EC as an example, the EC concentrations are mostly accounted for by the three combustion factors, i.e., vehicular emissions (GZ: 45 %, NS: 14 %), biomass burning (GZ: 22 %, NS: 23 %), and ship emissions (GZ: 18 %, NS: 43 %). We also note that the HULIS-C/OC ratio in the BB factor was 0.16, in excellent agreement with the measured ratio (0.19 ± 0.03) reported for emissions of rice straw burning in a number of field and chamber experiments (Lin et al., 2010b).

3.2.3 Source apportionment of HULIS-C

HULIS are present in three of the six factors resolved by PMF, that is, secondary process, biomass burning, and ship emissions and sea salt aerosols. The other three factors did not contribute to HULIS. Table 2 shows the average factor contributions of HULIS-C. Figure 6 shows the spatial and temporal variation of individual factor contributions to HULIS-C.

Overall, secondary formation process was the most important source of HULIS throughout the year. On annual average, this factor contributed 69 % ($1.76 \mu\text{gC m}^{-3}$) and 55 % ($1.37 \mu\text{gC m}^{-3}$) to HULIS-C in GZ and NS, and the seasonal average was in the range of 49–82 % at the two sites, consistent with the high correlation between HULIS and the secondary inorganic species shown earlier. Several secondary formation processes, such as aqueous-phase oxidation and heterogeneous reactions, have been demonstrated in laboratory or smog chamber studies to produce HULIS (e.g., Hoffer et al., 2004; Holmes and Petrucci, 2006; Surratt et al., 2008). Sulfation processes involving heterogeneous reac-

tions of oxidation products of biogenic volatile organic compounds (BVOCs) (e.g., isoprene, α -pinene, β -pinene, and limonene, etc) with sulfate aerosol have been shown in both chamber and field studies to form organosulfates (e.g., Surratt et al., 2008), which are an important class of compounds in the HULIS fraction (e.g., Lin et al., 2012b). Both sulfate aerosol and BVOCs are abundant in the PRD, a subtropical and economically more developed region in China. The higher emissions of BVOCs in summer could possibly contribute to the higher HULIS concentrations in this season. In addition to organosulfates, numerous other oxygenated or nitrated organic compound formulas are reported to be HULIS constituents (Lin et al., 2012a), but their formation processes or precursors are much less understood.

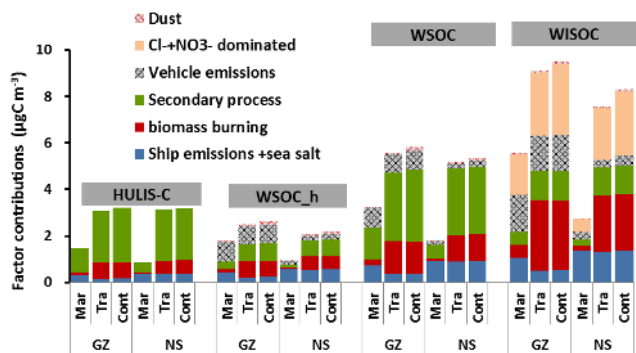
Biomass burning was also a significant contributor to HULIS-C with strong seasonal variation. Its percent contributions in winter (GZ: 28 %, NS: 20 %) were roughly 2–3 times those in summer (GZ: 11 %, NS: 8 %) while the mass contributions in winter (GZ: 1.02 , NS: $0.68 \mu\text{gC m}^{-3}$) were 5–6 times those in summer (GZ: 0.17 , NS: $0.10 \mu\text{gC m}^{-3}$). The seasonal contrast of BB contributions was a reflection of the seasonal patterns of BB activities in this region. BB contributions were also significant in spring 2009 (GZ: 25 %, NS: 21 %).

The above source apportionment results are consistent with qualitative evidence by other studies reporting that secondary formation process and BB were important HULIS sources (Altieri et al., 2008; El Haddad et al., 2011; Lin et al., 2010a). However, it is an unexpected result that this PMF analysis identifies ship emissions and sea salt factor as a source for HULIS-C. There were no prior studies reporting such a HULIS source. Nor was this hinted by the interspecies correlation analysis (Table S2).

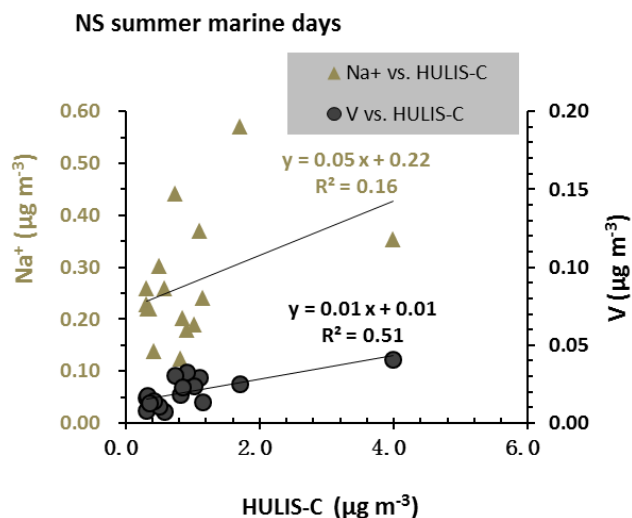
The PMF analysis apportioned a seasonal average of HULIS-C in the range of 0.21 – $0.35 \mu\text{gC m}^{-3}$ (7–19 %) at GZ and 0.52 – $0.84 \mu\text{gC m}^{-3}$ (21–44 %) at NS to the ship emissions and sea salt aerosols factor. The factor contributions at NS were consistently higher than those at GZ in all seasons. As marked in Fig. 1, a shipping lane links the few large coastal ports (Kwai Chung Port in Hong Kong, Yantian and Shekou Ports in Shenzhen, Nansha Port in the estuary of the Pearl River) and extends along the Pearl River to the further inland ports (Xinsha Port, Huangpu Port and the Guangzhou Downtown Port). Ocean-going vessels usually stop at the coastal ports in Hong Kong and Shenzhen while river vessels travel along the Pearl River to deliver goods between the coastal and inland ports. Ng et al. (2012) examined SO_2 emissions from shipping industries in the PRD and found Kwai Chung, Yantian and Shekou to be the key ship emissions spots, as the ocean-going vessels are much more significant emitters of PM than river vessels due to their larger size and numbers. The closer proximity of the NS site to the shipping lane supports the finding of the higher contributions of shipping emissions at this site.

Table 2. Contribution to HULIS-C from individual sources and percentage of the total modeled HULIS-C

	Site	Average HULIS-C measured $\mu\text{gC m}^{-3}$	Biomass burning $\mu\text{gC m}^{-3}$	Secondary sulfate formation process $\mu\text{gC m}^{-3}$	Ship emissions & sea salt $\mu\text{gC m}^{-3}$
Mar–Apr	GZ	2.17 ± 0.77	$0.54 (25 \pm 20 \%)$	$1.36 (63 \pm 16 \%)$	$0.27 (12 \pm 14 \%)$
	NS	2.45 ± 0.65	$0.52 (21 \pm 15 \%)$	$1.41 (58 \pm 14 \%)$	$0.52 (21 \pm 9 \%)$
May–Aug	GZ	1.60 ± 0.99	$0.17 (11 \pm 10 \%)$	$1.12 (70 \pm 21 \%)$	$0.30 (19 \pm 12 \%)$
	NS	1.32 ± 1.37	$0.10 (8 \pm 11 \%)$	$0.64 (49 \pm 25 \%)$	$0.58 (44 \pm 21 \%)$
Sep–Oct	GZ	2.98 ± 1.39	$0.33 (11 \pm 7 \%)$	$2.44 (82 \pm 7 \%)$	$0.21 (7 \pm 8 \%)$
	NS	3.62 ± 2.22	$0.32 (9 \pm 6 \%)$	$2.50 (69 \pm 16 \%)$	$0.80 (22 \pm 21 \%)$
Nov–Feb	GZ	3.63 ± 2.44	$1.02 (28 \pm 14 \%)$	$2.26 (62 \pm 13 \%)$	$0.35 (10 \pm 13 \%)$
	NS	3.32 ± 2.02	$0.68 (20 \pm 14 \%)$	$1.80 (54 \pm 25 \%)$	$0.84 (25 \pm 32 \%)$
Whole year	GZ	2.54 ± 1.78	$0.45 (18 \pm 15 \%)$	$1.76 (69 \pm 17 \%)$	$0.33 (13 \pm 13 \%)$
	NS	2.44 ± 1.92	$0.33 (13 \pm 13 \%)$	$1.37 (55 \pm 23 \%)$	$0.77 (31 \pm 25 \%)$

**Figure 7.** Average source factor contributions to HULIS-C, hydrophilic WSOC (WSOC_h), WSOC, and water-insoluble organic carbon (WISOC) in samples under influence of different air masses (Mar represents marine; Tra represents transitional; Cont represents continental).

Chemical information also confirms that ship emissions contributed to HULIS when summer NS sampling days under marine air mass influence were pooled together for examination. This subset of sampling days were chosen as they were least influenced by the other two sources of HULIS (i.e., secondary formation and BB activities). This can be seen in Fig. 7, which shows the average factor contributions to HULIS-C under influence of different air masses. The contribution from secondary formation process was much lower on “marine” days (GZ: $1.05 \mu\text{g m}^{-3}$, NS: $0.44 \mu\text{g m}^{-3}$) than on “continental” days (GZ: $2.35 \mu\text{g m}^{-3}$, NS: $2.22 \mu\text{g m}^{-3}$). BB contribution was also much lower on “marine” days (GZ: $0.13 \mu\text{g m}^{-3}$, NS: $0.06 \mu\text{g m}^{-3}$) than on ‘continental’ days (GZ: $0.69 \mu\text{g m}^{-3}$, NS: $0.58 \mu\text{g m}^{-3}$). Both results could be explained as a result of the clean marine air mass low in secondary aerosol precursor and in pollution from BB sources. For the summer “marine” days at NS, the correlation coefficient (R^2) of HULIS-C vs. V (a tracer of residual oil combus-

**Figure 8.** Correlations of Na^+ and V with HULIS-C at NS on summer days under influences of air masses of marine origin.

tion that is characteristic of ship emissions (Kowalczyk et al., 1982; Chow and Watson, 2002)) was 0.51 while the correlation between HULIS-C and Na^+ was very weak ($R^2 = 0.16$) (Fig. 8). We note that the HULIS-C vs. V correlation was nearly zero when the whole data set was considered, as contribution of shipping emissions was masked by the other samples due to more significant contributions from the secondary process and BB source. The positive correlation between HULIS-C and V and lack of correlation between HULIS-C and Na^+ in the subset of the NS samples ($n = 16$) implicates shipping emissions, not sea salt, as a source of HULIS. Since the number of data points collected on the “marine” days in NS site is small, further studies are needed to collect more ambient samples affected by ship emissions to confirm the link between residual oil combustion emissions and HULIS.

The contribution from the ship emissions and sea salt source in GZ, was higher under the influence of marine air masses ($0.29 \mu\text{g m}^{-3}$) than under continental air masses ($0.15 \mu\text{g m}^{-3}$). But in NS, the average HULIS-C from ship emissions on “marine” and “continental” days were similar (both were $0.36 \mu\text{g m}^{-3}$). The significant difference between “marine” and “continental” days in GZ, as well as the lack of difference in NS, are reasonable in light of their relative distance to the container ports and the shipping lane.

Formation of HULIS during combustion of residual oil could be broadly envisioned as a result of incomplete combustion, similar to formation of HULIS during BB. The HULIS-C/OC ratios in these two combustion sources as resolved by the PMF analysis were similar (~ 0.16), suggesting the HULIS contents in OC from these two types of combustion aerosols are similar. It is interesting to note that vehicular emissions, the other combustion source, had little contribution to HULIS. This could be explained as a result of much more complete combustion and more advanced emission controls in vehicles. The presence of HULIS in coal combustion source samples is also detected (unpublished result from our group), supporting the suggestion that HULIS are commonly formed as a result of incomplete combustion. We note that sulfate appears in the ship emission source factor. This could be a result of primary emissions from sulfur-containing fuel constituents in the residual oil or that some of the primary ship emissions have been processed. As such, HULIS in the ship emission factor could be partly secondary products of ship emissions atmospheric aging.

3.2.4 Source apportionment of WSOC_h and WISOC

In the PMF analysis, WSOC_h and OC were included as input and consequently their source apportionment can be derived. The source apportionment of WSOC and WISOC are indirectly computed from individual factor source contributions of HULIS-C, WSOC_h, and OC. Figure 7 shows the source apportionment results for HULIS-C, WSOC_h, WSOC, and WISOC averaged for samples categorized by influencing air mass origins.

Hydrophilic WSOC was apportioned to all but one (the Cl^- and NO_3^- dominated factor) of the factors resolved by PMF. Unlike HULIS-C, vehicular emissions were identified to be a significant source to WSOC_h. The mass contribution of this source had little dependence on air mass origins while significant urban–suburban gradient was recorded, with its levels at GZ ($0.81\text{--}0.83 \mu\text{gC m}^{-3}$, 31–47%) much higher than at NS ($0.17\text{--}0.23 \mu\text{gC m}^{-3}$, 9–18%), consistent with the site characteristics. The source contribution contrast of vehicular emissions to HULIS-C and WSOC_h may reflect that high combustion efficiencies in vehicles more likely produce smaller and therefore more hydrophilic WSOC. Ship emissions and sea salt aerosol factor contributed similar amounts of WSOC_h (GZ: $0.21\text{--}0.43$; NS: $\sim 0.55 \mu\text{gC m}^{-3}$) and HULIS-C (GZ: $0.14\text{--}0.29$; NS: $\sim 0.36 \mu\text{gC m}^{-3}$). BB

also contributed similar amounts of HULIS-C and WSOC_h among samples influenced by air masses of the same origin, with the contributions much higher on “continental” days (GZ: $\sim 0.69 \mu\text{gC m}^{-3}$ and NS: $\sim 0.58 \mu\text{gC m}^{-3}$) and “transitional” days (GZ: $\sim 0.70 \mu\text{gC m}^{-3}$ and NS: $\sim 0.56 \mu\text{gC m}^{-3}$) than on “marine” days (GZ: $\sim 0.13 \mu\text{gC m}^{-3}$ and NS: $\sim 0.06 \mu\text{gC m}^{-3}$). The WSOC_h from secondary formation process was ~ 0.7 at NS and $\sim 0.74 \mu\text{gC m}^{-3}$ at GZ on “continental”/“transitional” days and 0.14 at NS and $0.33 \mu\text{gC m}^{-3}$ at GZ on ‘marine’ days. Secondary formation process produced more WSOC as HULIS-C than WSOC_h, with HULIS-C approximately 3 times WSOC_h for all three types of sampling days. This finding was in agreement with the observation by Miyazaki et al. (2009). They reported that when aerosols aged for 10 h (the age was based on the NO_x/NO_y ratio), hydrophobic WSOC (roughly equivalent to HULIS-C in this work) increased by a factor of 5, while hydrophilic WSOC increased by only a factor of 2 to 3.

WSOC, the sum of HULIS-C and WSOC_h, was more frequently measured in past studies (e.g., Huang et al., 2006; Kondo et al., 2007; Duong et al., 2011; Zhang et al., 2012; Li et al., 2013). Secondary formation and BB are two commonly recognized sources for WSOC through field measurements. Our results confirm this consensus, with 32–56% of WSOC accounted for by secondary formation and 6–25% by BB on sampling days under influence of different air masses (Fig. 7).

WISOC was apportioned to all factors resolved by PMF. The dust factor was a very minor contributor ($< 3\%$). The contributions from the other five factors were roughly comparable on “continental”/“transitional” days while more varied on “marine” days (Fig. 7). WISOC had moderate correlations with EC, with $R^2 = 0.51$ at GZ and 0.74 at NS (Fig. S4), suggesting primary combustion sources as the main suppliers of WISOC in $\text{PM}_{2.5}$. We note that a sizable portion of WISOC was apportioned to the Cl^- and NO_3^- dominated factor. We are unclear about the underlying source or formation processes.

4 Summary and conclusions

This study is the first of its kind to apportion sources contributing to HULIS through PMF modeling of $\text{PM}_{2.5}$ major constituents and key source tracers. The observation sites are one urban (GZ) and one suburban location (NS) in the Pearl River Delta, one of the economically most developed region in China and also a region home to an active shipping industry. Six source factors were identified. Among them, secondary process, biomass burning and residual oil combustion (ship emissions) were found to contribute to HULIS. The secondary process factor contributed most to HULIS-C, with an average seasonal contribution of 49–82% or an average of $\sim 70\%$ on sampling days under influences of continental or transitional air masses. Biomass burning was an important

contributor in winter, contributing 20 and 28 % of HULIS-C in NS and GZ, respectively. Residual oil combustion from shipping was for the first time identified to be an important primary source for HULIS, its contributions comparable or exceeding those from BB at the NS site due to its proximity to the container ports and shipping lane in the region.

Vehicular emissions, unlike the other two combustion sources (i.e., residual oil combustion and BB), was not a contributor to HULIS while this source was a supplier of the hydrophilic WSOC. The contrast in contributions to HULIS by different combustion sources led us to postulate that HULIS are a common group of products of inefficient combustion processes while more efficient combustion processes (such as internal combustion in vehicles) produces little HULIS. Future studies are suggested to focus on the mechanism of HULIS formation and chemical characteristics from the three identified sources.

The Supplement related to this article is available online at doi:10.5194/acp-15-1995-2015-supplement.

Acknowledgements. This work was partially supported by Natural Science Foundation of China (21177031), NSFC-GD Joint Funding Key Project (U1033001), and the Research Grants Council of Hong Kong (621312). We gratefully acknowledge the Fok Ying Tung Foundation for funding to the Atmospheric Research Center (ARC) at HKUST Fok Ying Tung Graduate School, enabling sample collection at Nansha and Guangzhou. We thank the sampling and analysis team at ARC for sample collection and analysis of aerosol major constituents, QiongQiong Wang for assisting with the TD-GCMS analysis and Stephen Griffith for editing the paper.

Edited by: A. Laskin

References

- Altieri, K. E., Seitzinger, S. P., Carlton, A. G., Turpin, B. J., Klein, G. C., and Marshall, A. G.: Oligomers formed through in-cloud methylglyoxal reactions: Chemical composition, properties, and mechanisms investigated by ultra-high resolution FT-ICR mass spectrometry, *Atmos. Environ.*, 42, 1476–1490, doi:10.1016/j.atmosenv.2007.11.015, 2008.
- Cavalli, F., Facchini, M. C., Decesari, S., Mircea, M., Emblico, L., Fuzzi, S., Ceburnis, D., Yoon, Y. J., O'Dowd, C. D., Putaud, J. P., and Dell'Acqua, A.: Advances in characterization of size-resolved organic matter in marine aerosol over the North Atlantic, *J. Geophys. Res.-Atmos.*, 109, D24215, doi:10.1029/2004jd005137, 2004.
- Chow, J. C. and Watson, J. G.: Review of PM_{2.5} and PM₁₀ apportionment of fossil fuel combustion and other sources by chemical mass balance receptor model, *Energy Fuels*, 16, 222–260, doi:10.1021/ef0101715, 2002.
- Decesari, S., Facchini, M. C., Fuzzi, S., and Tagliavini, E.: Characterization of water-soluble organic compounds in atmospheric aerosol: A new approach, *J. Geophys. Res.-Atmos.*, 105, 1481–1489, doi:10.1029/1999jd900950, 2000.
- Dinar, E., Taraniuk, I., Graber, E. R., Katsman, S., Moise, T., Anttila, T., Mentel, T. F., and Rudich, Y.: Cloud Condensation Nuclei properties of model and atmospheric HULIS, *Atmos. Chem. Phys.*, 6, 2465–2481, doi:10.5194/acp-6-2465-2006, 2006.
- Ding, X., Wang, X. M., Gao, B., Fu, X. X., He, Q. F., Zhao, X. Y., Yu, J. Z., and Zheng, M.: Tracer-based estimation of secondary organic carbon in the Pearl River Delta, south China, *J. Geophys. Res.-Atmos.*, 117, D05313, doi:10.1029/2011jd016596, 2012.
- Draxler, R. R. and Rolph, G. D.: HYSPLIT (HYbrid Single-Particle Lagrangian Integrated Trajectory) Model access via NOAA ARL READY Website (<http://www.arl.noaa.gov/HYSPLIT.php>). NOAA Air Resources Laboratory, College Park, MD., 2011.
- Duong, H. T., Sorooshian, A., Craven, J. S., Hersey, S. P., Metcalf, A. R., Zhang, X. L., Weber, R. J., Jonsson, H., Flagan, R. C., and Seinfeld, J. H.: Water-soluble organic aerosol in the Los Angeles Basin and outflow regions: Airborne and ground measurements during the 2010 CalNex field campaign, *J. Geophys. Res.-Atmos.*, 116, D00V04, doi:10.1029/2011JD016674, 2011.
- El Haddad, I., Marchand, N., Temime-Roussel, B., Wortham, H., Piot, C., Besombes, J. L., Baduel, C., Voisin, D., Armengaud, A., and Jaffrezo, J. L.: Insights into the secondary fraction of the organic aerosol in a Mediterranean urban area: Marseille, *Atmos. Chem. Phys.*, 11, 2059–2079, doi:10.5194/acp-11-2059-2011, 2011.
- Engling, G., Carrico, C. M., Kreidenweis, S. M., Collett, J. L., Day, D. E., Malm, W. C., Lincoln, E., Hao, W. M., Iinuma, Y., and Herrmann, H.: Determination of levoglucosan in biomass combustion aerosol by high-performance anion-exchange chromatography with pulsed amperometric detection, *Atmos. Environ.*, 40, S299–S311, doi:10.1016/j.atmosenv.2005.12.069, 2006.
- Guo, H., Ding, A. J., So, K. L., Ayoko, G., Li, Y. S., and Hung, W. T.: Receptor modeling of source apportionment of Hong Kong aerosols and the implication of urban and regional contribution, *Atmos. Environ.*, 43, 1159–1169, doi:10.1016/j.atmosenv.2008.04.046, 2009.
- Graber, E. R. and Rudich, Y.: Atmospheric HULIS: How humic-like are they? A comprehensive and critical review, *Atmos. Chem. Phys.*, 6, 729–753, doi:10.5194/acp-6-729-2006, 2006.
- Harrison, R. M., Beddows, D. C. S., Hu, L., and Yin, J.: Comparison of methods for evaluation of wood smoke and estimation of UK ambient concentrations, *Atmos. Chem. Phys.*, 12, 8271–8283, doi:10.5194/acp-12-8271-2012, 2012.
- Havers, N., Burba, P., Klockow, D., and Klockow-Beck, A.: Characterization of humic-like substances in airborne particulate matter by capillary electrophoresis, *Chromatographia*, 47, 619–624, doi:10.1007/Bf02467443, 1998a.
- Havers, N., Burba, P., Lambert, J., and Klockow, D.: Spectroscopic characterization of humic-like substances in airborne particulate matter, *J. Atmos. Chem.*, 29, 45–54, doi:10.1023/A:1005875225800, 1998b.
- Ho, S. S. H. and Yu, J. Z.: In-Injection Port Thermal Desorption and Subsequent Gas Chromatography-Mass Spectrometric Analysis

- of Polycyclic Aromatic Hydrocarbons and n-Alkanes in Atmospheric Aerosol Samples, *J. Chromatography A*, 1059, 121–129, doi:10.1016/j.chroma.2004.10.013, 2004.
- Ho, S. S. H., Yu, J. Z., Chow, J. C., Watson, J. G., Zielinska, B., Watson, J. G., Sit, E. H. L., and Schauer, J. J.: Evaluation of an In-Injection Port Thermal Desorption GC-MS Method for Analysis of Non-polar Organic Compounds in Ambient Aerosol Samples, *J. Chromatography A*, 1200, 217–227, doi:10.1016/j.chroma.2008.05.056, 2008.
- Hoffer, A., Kiss, G., Blazso, M., Gelencser, A.: Chemical characterization of humic-like substances (HULIS) formed from a lignin-type precursor in model cloud water, *Geophys. Res. Lett.*, 31, L06115, doi:10.1029/2003GL018962, 2004.
- Hoffer, A., Gelencser, A., Guyon, P., Kiss, G., Schmid, O., Frank, G. P., Artaxo, P., and Andreae, M. O.: Optical properties of humic-like substances (HULIS) in biomass-burning aerosols, *Atmos. Chem. Phys.*, 6, 3563–3570, doi:10.5194/acp-6-3563-2006, 2006.
- Holden, A. S., Sullivan, A. P., Munchak, L. A., Kreidenweis, S. M., Schichtel, B. A., Malm, W. C., and Collett, J. L.: Determining contributions of biomass burning and other sources to fine particle contemporary carbon in the western United States, *Atmos. Environ.*, 45, 1986–1993, doi:10.1016/j.atmosenv.2011.01.021, 2011.
- Holmes, B. J. and Petrucci, G. A.: Water-soluble oligomer formation from acid-catalyzed reactions of levoglucosan in proxies of atmospheric aqueous aerosols, *Environ. Sci. Technol.*, 40, 4983–4989, doi:10.1021/es060646c, 2006.
- Hu, D., Bian, Q. J., Lau, A. K. H., and Yu, J. Z.: Source apportionment of primary and secondary organic carbon in summer PM_{2.5} in Hong Kong using positive matrix factorization of secondary and primary organic tracer data, *J. Geophys. Res.-Atmos.*, 115, D16204, doi:10.1029/2009jd012498, 2010.
- Huang, X. F., Yu, J. Z., He, L. Y., and Yuan, Z. B.: Water-soluble organic carbon and oxalate in aerosols at a coastal urban site in China: Size distribution characteristics, sources, and formation mechanisms, *J. Geophys. Res.-Atmos.*, 111, D22212, doi:10.1029/2006jd007408, 2006.
- Huang, X. H. H., Bian, Q., Ng, W. M., Louie, P. K. K., and Yu, J. Z.: Characterization of PM_{2.5} major components and source investigation in suburban Hong Kong: a one year monitoring study, *Aerosol Air Qual. Res.*, 14, 237–250, doi:10.4209/aaqr.2013.01.0020, 2014.
- Khan, M. F., Hirano, K., and Masunaga, S.: Assessment of the sources of suspended particulate matter aerosol using US EPA PMF 3.0, *Environ. Monit. Assess.*, 184, 1063–1083, doi:10.1007/s10661-011-2021-y, 2012.
- Kim, E. and Hopke, P. K.: Source apportionment of fine particles in Washington, DC, utilizing temperature-resolved carbon fractions, *J. Air Waste Manage.*, 54, 773–785, doi:10.1080/10473289.2004.10470948, 2004.
- Kim, E. and Hopke, P. K.: Source identifications of airborne fine particles using positive matrix factorization and US environmental protection agency positive matrix factorization, *J. Air Waste Manage.*, 57, 811–819, doi:10.3155/1047-3289.57.7.811, 2007.
- Kim, E., Turkiewicz, K., Zulawnick, S. A., and Magliano, K. L.: Sources of fine particles in the South Coast area, California, *Atmos. Environ.*, 44, 3095–3100, doi:10.1016/j.atmosenv.2010.05.037, 2010.
- Kiss, G., Varga, B., Galambos, I., and Ganszky, I.: Characterization of water-soluble organic matter isolated from atmospheric fine aerosol, *J. Geophys. Res.-Atmos.*, 107, 8339, doi:10.1029/2001jd000603, 2002.
- Kiss, G., Tombacz, E., and Hansson, H. C.: Surface tension effects of humic-like substances in the aqueous extract of tropospheric fine aerosol, *J. Atmos. Chem.*, 50, 279–294, doi:10.1007/s10874-005-5079-5, 2005.
- Kondo, Y., Miyazaki, Y., Takegawa, N., Miyakawa, T., Weber, R. J., Jimenez, J. L., Zhang, Q., and Worsnop, D. R.: Oxygenated and water-soluble organic aerosols in Tokyo, *J. Geophys. Res.-Atmos.*, 112, D01203, doi:10.1029/2006JD007056, 2007.
- Kowalczyk, G. S., Gordon, G. E., and Rheingrover, S. W.: Identification of atmospheric particulate sources in Washington D.C. using chemical element balances, *Environ. Sci. Technol.*, 16, 79–90, doi:10.1021/es00096a005, 1982.
- Krivacsy, Z., Kiss, G., Varga, B., Galambos, I., Sarvari, Z., Gelencser, A., Molnar, A., Fuzzi, S., Facchini, M. C., Zappoli, S., Andracchio, A., Alsberg, T., Hansson, H. C., and Persson, L.: Study of humic-like substances in fog and interstitial aerosol by size-exclusion chromatography and capillary electrophoresis, *Atmos. Environ.*, 34, 4273–4281, doi:10.1016/S1352-2310(00)00211-9, 2000.
- Krivacsy, Z., Kiss, G., Ceburnis, D., Jennings, G., Maenhaut, W., Salma, I., and Shooter, D.: Study of water-soluble atmospheric humic matter in urban and marine environments, *Atmos. Res.*, 87, 1–12, doi:10.1016/j.atmosres.2007.04.005, 2008.
- Lee, E., Chan, C. K., and Paatero, P.: Application of positive matrix factorization in source apportionment of particulate pollutants in Hong Kong, *Atmos. Environ.*, 33, 3201–3212, doi:10.1016/S1352-2310(99)00113-2, 1999.
- Li, Y. C., Yu, J. Z., Ho, S. S. H., Schauer, J. J., Yuan, Z. B., Lau, A. K. H., and Louie, P. K. K.: Chemical characteristics and source apportionment of fine particulate organic carbon in Hong Kong during high particulate matter episodes in winter 2003, *Atmos. Res.*, 120–121, 88–98, doi:10.1016/j.atmosres.2012.08.005, 2013.
- Lin, P., Huang, X. F., He, L. Y., and Yu, J. Z.: Abundance and size distribution of HULIS in ambient aerosols at a rural site in South China, *J. Aerosol. Sci.*, 41, 74–87, doi:10.1016/j.jaerosci.2009.09.001, 2010a.
- Lin, P., Engling, G., and Yu, J. Z.: Humic-like substances in fresh emissions of rice straw burning and in ambient aerosols in the Pearl River Delta Region, China, *Atmos. Chem. Phys.*, 10, 6487–6500, doi:10.5194/acp-10-6487-2010, 2010b.
- Lin, P. and Yu, J. Z.: Generation of Reactive Oxygen Species Mediated by Humic-like Substances in Atmospheric Aerosols, *Environ. Sci. Technol.*, 45, 10362–10368, doi:10.1021/Es2028229, 2011.
- Lin, P., Rincon, A. G., Kalberer, M., Yu, J. Z.: Elemental Composition of HULIS in the Pearl River Delta Region, China: Results Inferred from Positive and Negative Electrospray High Resolution Mass Spectrometric Data, *Environ. Sci. Technol.*, 46, 7454–7462, doi:10.1021/es300285d, 2012a.
- Lin, P., Yu, J. Z., Engling, G., and Kalberer, M.: Organosulfates in humic-like substance fraction isolated from aerosols at seven locations in East Asia: A study by ultrahigh resolution mass spectrometry, *Environ. Sci. Technol.*, 46, 13118–13127, doi:10.1021/es303570v, 2012b.

- Liu, W., Wang, Y. H., Russell, A., and Edgerton, E. S.: Atmospheric aerosol over two urban-rural pairs in the southeastern United States: Chemical composition and possible sources, *Atmos. Environ.*, 39, 4453–4470, doi:10.1016/j.atmosenv.2005.03.048, 2005.
- Lukacs, H., Gelencser, A., Hammer, S., Puxbaum, H., Pio, C., Legrand, M., Kasper-Giebl, A., Handler, M., Limbeck, A., Simpson, D., and Preunkert, S.: Seasonal trends and possible sources of brown carbon based on 2-year aerosol measurements at six sites in Europe, *J. Geophys. Res.-Atmos.*, 112, D23s18, doi:10.1029/2006jd008151, 2007.
- Maykut, N. N., Lewtas, J., Kim, E., and Larson, T. V.: Source apportionment of PM_{2.5} at an urban IMPROVE site in Seattle, Washington, *Environ. Sci. Technol.*, 37, 5135–5142, doi:10.1021/Es030370y, 2003.
- Mayol-Bracero, O. L., Guyon, P., Graham, B., Roberts, G., Andreae, M. O., Decesari, S., Facchini, M. C., Fuzzi, S., and Artaxo, P.: Water-soluble organic compounds in biomass burning aerosols over Amazonia – 2. Apportionment of the chemical composition and importance of the polyacidic fraction, *J. Geophys. Res.-Atmos.*, 107, 8091, doi:10.1029/2001jd000522, 2002.
- Miyazaki, Y., Kondo, Y., Shiraiwa, M., Takegawa, N., Miyakawa, T., Han, S., Kita, K., Hu, M., Deng, Z. Q., Zhao, Y., Sugimoto, N., Blake, D. R., and Weber, R. J.: Chemical characterization of water-soluble organic carbon aerosols at a rural site in the Pearl River Delta, China, in the summer of 2006, *J. Geophys. Res.-Atmos.*, 114, D14208, doi:10.1029/2009JD011736, 2009.
- Mooibroek, D., Schaap, M., Weijers, E. P., and Hoogerbrugge, R.: Source apportionment and spatial variability of PM_{2.5} using measurements at five sites in the Netherlands, *Atmos. Environ.*, 45, 4180–4191, doi:10.1016/j.atmosenv.2011.05.017, 2011.
- Ng, S. K. W., Lin, C., Chan, J. W. M., Yip, A. C. K., Lau, A. K. H., Fung, J. C. H., Wu, D., and Li, Y.: Marine Vessel Smoke Emissions in Hong Kong and the Pearl River Delta, Final Report, available at: http://shipsairpollution.cleartheair.org.hk/wp-content/uploads/2013/08/201209FinalReport_hkust.pdf (last access: 7 August 2014), 2012.
- Nolte, C. G., Schauer, J. J., Cass, G. R., and Simoneit, B. R. T.: Highly polar organic compounds present in wood smoke and in the ambient atmosphere, *Environ. Sci. Technol.*, 35, 1912–1919, doi:10.1021/Es001420r, 2001.
- Norris, G., Vedantham, R., Wade, K., Brown, S., Prouty, J., and Foley, C.: EPA Positive Matrix Factorization (PMF) 3.0 Fundamentals & User Guide, EPA 600/R-08/108 ed., available at: www.epa.gov (last access: 22 September 2012), 2008.
- Polissar, A. V., Hopke, P. K., and Paatero, P.: Atmospheric aerosol over Alaska – 2. Elemental composition and sources, *J. Geophys. Res.-Atmos.*, 103, 19045–19057, doi:10.1029/98jd01212, 1998.
- Reff, A., Eberly, S. I., and Bhave, P. V.: Receptor modeling of ambient particulate matter data using positive matrix factorization: Review of existing methods, *J. Air Waste Manage.*, 57, 146–154, doi:10.1080/10473289.2007.10465319, 2007.
- Samburova, V., Szidat, S., Hueglin, C., Fisseha, R., Baltensperger, U., Zenobi, R., and Kalberer, M.: Seasonal variation of high-molecular-weight compounds in the water-soluble fraction of organic urban aerosols, *J. Geophys. Res.-Atmos.*, 110, D23210, doi:10.1029/2005jd005910, 2005a.
- Samburova, V., Zenobi, R., and Kalberer, M.: Characterization of high molecular weight compounds in urban atmospheric particles, *Atmos. Chem. Phys.*, 5, 2163–2170, doi:10.5194/acp-5-2163-2005, 2005b.
- Shrivastava, M. K., Subramanian, R., Rogge, W. F., and Robinson, A. L.: Sources of organic aerosol: Positive matrix factorization of molecular marker data and comparison of results from different source apportionment models, *Atmos. Environ.*, 41, 9353–9369, doi:10.1016/j.atmosenv.2007.09.016, 2007.
- Simoneit, B. R. T.: Organic matter of the troposphere – III. Characterization and sources of petroleum and pyrogenic residues in aerosols over the western United States, *Atmos. Environ.*, 18, 51–67, doi:10.1016/0004-6981(84)90228-2, 1984.
- Simoneit, B. R. T., Schauer, J. J., Nolte, C. G., Oros, D. R., Elias, V. O., Fraser, M. P., Rogge, W. F., and Cass, G. R.: Levoglucosan, a tracer for cellulose in biomass burning and atmospheric particles, *Atmos. Environ.*, 33, 173–182, doi:10.1016/S1352-2310(98)00145-9, 1999.
- Surratt, J. D., Gómez-González, Y., Chan, A. W., Vermeylen, R., Shahgholi, M., Kleindienst, T. E., and Seinfeld, J. H.: Organosulfate formation in biogenic secondary organic aerosol, *J. Phys. Chem. A*, 112, 8345–8378, doi:10.1021/jp802310p, 2008.
- Varga, B., Kiss, G., Ganszky, I., Gelencser, A., and Krivacsy, Z.: Isolation of water-soluble organic matter from atmospheric aerosol, *Talanta*, 55, 561–572, doi:10.1016/S0039-9140(01)00446-5, 2001.
- Verma, V., Rico-Martinez, R., Kotra, N., King, L., Liu, J. M., Snell, T. W., and Weber, R. J.: Contribution of Water-Soluble and Insoluble Components and Their Hydrophobic/Hydrophilic Sub-fractions to the Reactive Oxygen Species-Generating Potential of Fine Ambient Aerosols, *Environ. Sci. Technol.*, 46, 11384–11392, doi:10.1021/Es302484r, 2012.
- Wagener, S., Langner, M., Hansen, U., Moriske, H. J., and Endlicher, W. R.: Source apportionment of organic compounds in Berlin using positive matrix factorization - Assessing the impact of biogenic aerosol and biomass burning on urban particulate matter, *Sci. Total Environ.*, 435, 392–401, doi:10.1016/j.scitotenv.2012.07.039, 2012.
- Wang, Q. Q., Shao, M., Liu, Y., William, K., Paul, G., Li, X. H., Liu, Y. A., and Lu, S. H.: Impact of biomass burning on urban air quality estimated by organic tracers: Guangzhou and Beijing as cases, *Atmos. Environ.*, 41, 8380–8390, doi:10.1016/j.atmosenv.2007.06.048, 2007.
- Wang, Y. G., Hopke, P. K., Xia, X. Y., Rattigan, O. V., Chalupa, D. C., and Utell, M. J.: Source apportionment of airborne particulate matter using inorganic and organic species as tracers, *Atmos. Environ.*, 55, 525–532, doi:10.1016/j.atmosenv.2012.03.073, 2012.
- Wozniak, A. S., Bauer, J. E., Sleighter, R. L., Dickhut, R. M., & Hatcher, P. G.: Technical Note: Molecular characterization of aerosol-derived water soluble organic carbon using ultrahigh resolution electrospray ionization Fourier transform ion cyclotron resonance mass spectrometry, *Atmos. Chem. Phys.*, 8, 5099–5111, doi:10.5194/acp-8-5099-2008, 2008.
- Wu, C., Ng, W. M., Huang, J. X., Wu, D., and Yu, J. Z.: Determination of Elemental and Organic Carbon in PM_{2.5} in the Pearl River Delta Region: Inter-Instrument (Sunset vs. DRI Model 2001 Thermal/Optical Carbon Analyzer) and Inter-Protocol Comparisons (IMPROVE vs. ACE-Asia Protocol), *Aerosol Sci. Tech.*, 46, 610–621, doi:10.1080/02786826.2011.649313, 2012.
- Yang, H., Yu, J. Z., Ho, S. S. H., Xu, J. H., Wu, W. S., Wan, C. H., Wang, X. D., Wang, X. R., and Wang, L. S.: The chem-

- ical composition of inorganic and carbonaceous materials in PM_{2.5} in Nanjing, China, *Atmos. Environ.*, 39, 3735–3749, doi:10.1016/j.atmosenv.2005.03.010, 2005.
- Yassine, M. M., Dabek-Zlotorzynska, E., Harir, M., and Schmitt-Kopplin, P.: Identification of Weak and Strong Organic Acids in Atmospheric Aerosols by Capillary Electrophoresis/Mass Spectrometry and Ultra-High-Resolution Fourier Transform Ion Cyclotron Resonance Mass Spectrometry, *Anal. Chem.*, 84, 6586–6594, doi:10.1021/ac300798g, 2012.
- Yu, J. Z., Huang, X. F., Xu, J. H., and Hu, M.: When aerosol sulfate goes up, so does oxalate: Implication for the formation mechanisms of oxalate, *Environ. Sci. Technol.*, 39, 128–133, doi:10.1021/es049559f, 2005.
- Yuan, Z. B., Lau, A. K. H., Zhang, H. Y., Yu, J. Z., Louie, P. K. K., and Fung, J. C. H.: Identification and spatiotemporal variations of dominant PM₁₀ sources over Hong Kong, *Atmos. Environ.*, 40, 1803–1815, doi:10.1016/j.atmosenv.2005.11.030, 2006a.
- Yuan, Z. B., Yu, J. Z., Lau, A. K. H., Louie, P. K. K., and Fung, J. C. H.: Application of positive matrix factorization in estimating aerosol secondary organic carbon in Hong Kong and its relationship with secondary sulfate, *Atmos. Chem. Phys.*, 6, 25–34, doi:10.5194/acp-6-25-2006, 2006b.
- Zhang, X., Liu, Z., Hecobian, A., Zheng, M., Frank, N. H., Edgerton, S., and Weber, R. J.: Spatial and seasonal variations of fine particle water-soluble organic carbon (WSOC) over the southeastern United States: implications for secondary organic aerosol formation, *Atmos. Chem. Phys.*, 12, 6593–6607, doi:10.5194/acp-12-6593-2012, 2012.
- Zota, A. R., Willis, R., Jim, R., Norris, G. A., Shine, J. P., Duvall, R. M., Schaidler, L. A., and Spengler, J. D.: Impact of Mine Waste on Airborne Respirable Particulates in Northeastern Oklahoma, United States, *J. Air Waste Manage.*, 59, 1347–1357, doi:10.3155/1047-3289.59.11.1347, 2009.